Int. J. Heat Mass Transfer. Vol. 14, pp. 1395–1405. Pergamon Press 1971. Printed in Great Britain

HEAT TRANSFER TO BINARY MIST FLOW

J. W. HEYT

Department of Mechanical Engineering, The University of Texas at Austin, Austin, Texas 78712, U.S.A.

and

P. S. LARSEN

Technical University of Denmark, Copenhagen, Denmark

(*Received* 15 *June* 1970 *and in revised form* 30 *November* 1970)

Abstract—The forced convection laminar boundary layer involving a two component gas with dispersed liquid particles over a dry isothermal surface is studied analytically and experimentally. The effect of particle presence and evaporation on boundary layer structure, wall heat transfer, and wall shear stress is determined for the limiting case of dilute concentrations of small particles having large evaporation rate. Solutions include distributions of velocity, temperature, vapor and liquid throughout the boundary layer and the extent of the region near the wall free of particles due to complete evaporation. It is shown that for increasing free stream liquid content the increase in wall heat transfer is substantial while that of wall shear is negligible. Theoretical results correlate wall heat transfer measurements for an air/water vapor, water particle mist flow.

NOMENCLATURE

The superscript * refers to the dimensional value; symbols without other notation refer to the gas phase.

C^p, C^g, C^v, constant pressure specific heat, $C^{p*}/C^*, C^{g*}/C^*, C^{v*}/C^*$;

C_1, C_2, C_3, constants in particle temperature equation, given in appendix;

D, particle diameter, D^*/D^*_∞;

$\bar{D}$, mean particle diameter, $\bar{D}^*/\bar{D}^*_\infty$;

D^*_{vg}, mass diffusivity of vapor in noncondensible gas;

E_1, E_2, variable coefficients, given in Appendix;

Ev, evaporation number, $h^*_{fg}/C^*(T^*_w - T^*_\infty)$;

f, transformed steam function;

F, particle size distribution function, $F^*\bar{D}_\infty/\bar{n}_\infty$;

g, transformed particle mass concentration;

h, transformed vapor mass concentration;

h^*_{fg}, liquid enthalpy of evaporation;

h^*, local heat transfer coefficient;

k^*, thermal conductivity;

L^*, characteristic plate length;

Lu, Lukomsky number, Pr/Sc;

$\bar{n}$, mean particle number concentration, $\bar{n}^*/\bar{n}^*_\infty$;

Nu, Nusselt number, h^*x^*/k^*;

Pr, Prandtl number, ν^*/α^*;

q^*, local heat flux;

$R, \tilde{R}$, liquid mass ratio, $\omega^{p*}_\infty/\rho^*, R(1 - \rho^*/\rho^{p*})$;

$Re, \tilde{Re}$, Reynolds number, $u^*_\infty L^*/\nu^*, u^*_\infty x^*/\nu^*$;

Sc, Schmidt number, ν^*/D^*_{vg};

S_1, S_2, variable coefficients, given in Appendix;

T, temperature, $(T^* - T^*_\infty)/(T^*_w - T^*_\infty)$;

u, x direction velocity, u^*/u^*_∞;
v, y direction velocity, v^*/u^*_∞;
x, coordinate along surface, x^*/L^*;
y, coordinate normal to surface, y^*/L^*.

Greek symbols

α^*, thermal diffusivity, $k^*/\rho^* C^*$;
δ, nondimensional inner boundary layer thickness;
η, similarity variable;
θ, transformed temperature;
λ^*, characteristic evaporation length, $\dfrac{\rho^{p*} u^*_\infty h^*_{fg} \bar{D}^{*2}_\infty}{8k^*(T^*_w - T^*_\infty)}$;
μ^*, dynamic viscosity;
ν^*, kinematic viscosity, μ^*/ρ^*;
ξ, transformed y coordinate;
$\hat{\rho}$, density, $\hat{\rho}^*/\rho^*$;
τ^*, local shear stress;
$\Phi_0, \Phi_1, \Phi_2, \ldots$, dependent variables in the solution;
χ, transformed x coordinate;
Ψ, stream function;
ω, ω^p, mass concentration, $\omega^{v*}/\rho^*, \omega^*/R\rho^{m*}$;
ω', constant in liquid vapor pressure equation, given in Appendix.

Subscripts

∞, free stream conditions;
w, wall conditions;
1, 2, 3---, order of terms in perturbation solution;
i, inner boundary layer region;
δ, interface between inner and outer regions.

Superscripts

g, noncondensible gas component;
p, particulate phase;
v, vapor component;
$\wedge$, mixture;
$'$, derivative.

INTRODUCTION

GAS FLOWS with suspended solid or liquid particles occur in numerous heat and mass transfer operations such as atomization and combustion of fuel, heat exchange processes utilizing multiphase fluids, and spray drying operations. In general, the distributed particles exchange momentum, energy, and mass with the continuous gas phase, resulting in a significant effect of the particles on temperature, velocity and concentration distributions throughout the gas phase and particulate cloud. Heat transfer and friction of the mixture on surrounding walls, criteria of primary importance in the design of heat exchange equipment and evaluation of a heat transfer fluid, are simultaneously altered by the particles. In the present investigation, the boundary layer on a heated surface subjected to forced convection mist flow, involving particles of a volatile liquid, is studied analytically and experimentally.

Gas boundary layers with suspended solid particles have been studied for incompressible [1] and compressible [2] flow in the absence of phase change. Velocity, temperature, and concentration distributions for both particles and gas have been determined for large values of the longitudinal coordinate. The boundary layer asymptotically approaches a limiting condition with no local velocity and temperature difference between phases, and the mixture behaves as a homogeneous fluid with properties dependent on particle mass fraction. For small values of the longitudinal coordinate, free stream conditions dominate particle behavior upon entering the boundary layer, and significant velocity and temperature differences between phases are predicted [3].

Mist flows involving liquid particles may be divided into two classes, characterized by the presence or absence of a liquid film on the boundary surface. Experiments [4, 5] and analytical studies [6, 7], dealing with the first class, which is realized at low wall temperature, have indicated an increase in heat transfer by a factor as high as 30 over that of single phase

gas flow. In this case the boundary layer is composed of two regions, an inner liquid layer on the solid surface and an outer two phase layer with distributed particles, between the liquid and free stream.

The second class of mist flows is realized for surface temperature high enough such that all liquid particles are evaporated before reaching the surface. Extensive attention has been directed toward determination of heat transfer in the presence of a dry wall for various internal flow regimes [8], also called the burnout or dryout condition. In the absence of constraining walls, however, an external boundary layer is formed, which is the subject of the present study.

The forced convection flow of a two phase mist over a dry, isothermal, heated surface is considered, with zero pressure gradient. The gas–liquid mixture is composed of a two component gas continuous phase with a single component liquid phase dispersed throughout in the form of tiny particles. One gas component is the vapor of the liquid, and the other component is noncondensible. The characteristic boundary layer structure of this flow is a result of shear which retards velocity near the wall, and diffusion of heat from the high temperature wall into the mixture, causing particle evaporation near the wall. The liquid evaporation causes a reduction in mixture density, with simultaneous absorption of latent heat and release of vapor. Since no particles collect on the wall, the presence of a single phase gas inner boundary layer region (void of particles) is indicated to be adjacent to the wall, in analogy to the vapor film adjacent to the wall in film boiling [9].

Compared to single phase gas flow, boundary layer temperatures in mist flow are reduced near the wall, primarily due to the absorption of latent heat upon particle evaporation, resulting in wall heat transfer increase. Although a change may be expected in skin friction due to the density change upon liquid evaporation, this effect is shown to be negligible at small free stream liquid content.

In the theoretical analysis, the conservation equations are written for momentum, energy, and mass concentration, resulting in the distributions of velocity, temperature and mass concentration throughout the boundary layer. Resulting wall heat flux and shear stress are also obtained. The experiment consists of measurements of wall heat flux in an air/water vapor, water particle mist flow over an isothermal heated surface with a zero pressure gradient.

THEORETICAL ANALYSIS

The boundary layer analysis is based on the following assumptions, which are valid for a Reynolds number range for incompressible single phase gas flow in the limiting case of small particles and low liquid mass concentration.

(1) Particles move with the local gas velocity.
(2) Particles undergo quasisteady evaporation from the local wet-bulb temperature.
(3) Particulate and gas phase density are each constant.
(4) Mixture transport properties are those of the gas alone.
(5) Collision, coalescence, and aerodynamic breakup of particles are negligible.

Under the boundary layer approximation, the governing differential equations are written in dimensionless form as follows:

Mixture continuity

$$\frac{\partial \hat{\rho} u}{\partial x} + \frac{\partial \hat{\rho} v}{\partial y} = 0, \tag{1}$$

Particulate phase continuity,

$$\frac{\partial Fu}{\partial x} + \frac{\partial Fv}{\partial y} - \frac{1}{2}\frac{L^*}{\lambda^*}(T^p - T)\frac{\partial}{\partial D}\left\{\frac{F}{D}\right\} = 0, \tag{2}$$

where L^*/λ^* is the ratio of characteristic flow length to the distance required for total evaporation of a particle of temperature T^*_∞, velocity u^*_∞, and initial size $\bar{D}^*_\infty$, in an environment of temperature T^*_w;

Vapor continuity,

$$u\frac{\partial\omega}{\partial x}+v\frac{\partial\omega}{\partial y}+R\hat{\rho}(1-\omega)\left\{u\frac{\partial\omega^p}{\partial x}-v\frac{\partial\omega^p}{\partial y}\right\}-\frac{1}{ReSc}\frac{\partial^2\omega}{\partial y^2}=0, \quad (3)$$

where R is the ratio of free stream particle mass concentration to continuous phase density, and Re and Sc denote the Reynolds and Schmidt number for single phase flow, respectively;

Mixture momentum,

$$\hat{\rho}\left\{u\frac{\partial u}{\partial x}+v\frac{\partial u}{\partial x}\right\}=\frac{1}{Re}\frac{\partial^2 u}{\partial y^2}, \quad (4)$$

Mixture energy,

$$u\frac{\partial T}{\partial x}+v\frac{\partial T}{\partial y}+R\hat{\rho}\omega^p C^p\left\{u\frac{\partial T^p}{\partial x}+v\frac{\partial T^p}{\partial y}\right\}-\frac{1}{ReSc}(C^v-C^g)\frac{\partial\omega}{\partial y}\frac{\partial T}{\partial y}+REv\left\{u\frac{\partial\omega^p}{\partial x}+v\frac{\partial\omega^p}{\partial y}\right\}=\frac{1}{RePr}\frac{\partial^2 T}{\partial y^2}, \quad (5)$$

where Ev is the ratio of the liquid latent heat of evaporation to the characteristic sensible heat of the gas phase. The parameters R, Ev and L^*/λ^* of this formulation are characteristic of two phase flows. In particular, the combination Ev appears in film condensation and boiling studies, and a length ratio analogous to L^*/λ^* has been identified with particulate flows not involving phase transformation (1).

For polydisperse mixtures characterized by the size distribution $F(x, y, D)$ giving the local number at particles of diameter D per unit volume, the liquid mass concentration is defined by

$$\omega^p=\frac{\int_0^\infty FD^3\,\mathrm{d}D}{1+\tilde{R}\int_0^\infty FD^3\,\mathrm{d}D}, \quad (6)$$

and the mixture density is defined by

$$\hat{\rho}=(1-\tilde{R}\omega^p)^{-1}. \quad (7)$$

Based on assumption 2, the local particle temperature is uniquely related to vapor temperature and concentration, written

$$T^p-T=C_1+C_2T+C_3\omega, \quad (8)$$

where the coefficients C_1, C_2, C_3, given in the appendix, are functions of Ev, Lu and ω_∞, ω'_∞, constants of the linearized particle vapor pressure curve which are also given in the appendix.

Boundary conditions for the particle size distribution are

$$F(x, y, 0)=0, \quad \lim_{y\to\infty}F(x, y, D)=F_\infty(D), \quad (9)$$

implying that no particles of zero diameter are present and the size distribution far from the surface is undisturbed. The other boundary conditions for an isothermal and impermeable wall are

$$u(x,0)=v(x,0)=T(x,0)=\frac{\partial\omega}{\partial y}(x,0)=0, \quad (10)$$

while in the undisturbed free stream,

$$\lim_{y\to\infty}\omega(x, y)=\omega_\infty, \quad \lim_{y\to\infty}u(x, y)=\lim_{y\to\infty}T(x, y)=1. \quad (11)$$

To arrive at equations (3) and (5), the moment of equation (2) with respect to $1/6\pi D^3\,\mathrm{d}D$ has been taken to yield the conservation equation for particle mass concentration,

$$\hat{\rho}\left\{u\frac{\partial\omega^p}{\partial x}+v\frac{\partial\omega^p}{\partial y}\right\}=-\frac{2}{3}\frac{L}{\lambda}\bar{n}\bar{D}(T^p-T) \quad (12)$$

where $\bar{D}$ and $\bar{n}$ denote the local average size and number concentration, respectively, as discussed by Shapiro and Erickson [10]. Equation (12) was then combined with the vapor continuity equation and the energy equation, replacing the mass generation terms with convection terms.

SOLUTION OF EQUATIONS

In view of the density variation of the flow, the coordinate transformation of Howarth and Stewartson [11] is employed to simplify

the formulation in conjunction with a stream function,

$$\hat{\rho}u = \frac{\partial \Psi}{\partial \chi}, \quad \hat{\rho}v = -\frac{\partial \Psi}{\partial y}, \tag{13}$$

$$\xi = \int_0^y \hat{\rho}\, dy, \quad \chi = x. \tag{14}$$

Next we consider the magnitude of the volume parameter λ^*/L^*, evaluated in Table 1 for typical conditions of water drops in air.

Table 1. Characteristic values of λ^*/L^* ($\rho^{p*} = 62{\cdot}4$ lbm/ft^3, $h_{fg}^* = 1000$ Btu/lbm, $k^* = 0{\cdot}01$ Btu/ft h F, $L^* = 1$ ft)

$\bar{D}^*$, microns	u_∞^*, ft/s	$T_w^* - T_\infty^*$, F	λ^*/L^*
1	10	250	0·00121
1	40	250	0·00484
10	10	250	0·121
10	40	250	0·484

Confining attention here to particles of small size of practical interest in mist flows, the dependent variables are expanded in a perturbation series in terms of the small parameter, λ^*/L^*,

$$\Phi(\chi, \xi, D, \lambda^*/L^*) = \Phi_0(\chi, \xi, D) + (\lambda^*/L^*)\,\Phi_1(\chi, \xi, D) + (\lambda^*/L^*)^2\,\Phi_2(\chi, \xi, D) + \ldots. \tag{15}$$

The resulting equations to order $(\lambda^*/L^*)^0$ are as follows, omitting the zero subscript.

$$T^p - T = 0, \tag{16}$$

$$R\hat{\rho}\{1 - \omega_\infty - \omega'_\infty(T - 1)\} \times \left\{\frac{\partial \Psi}{\partial \xi}\frac{\partial \omega^p}{\partial \chi} - \frac{\partial \Psi}{\partial \chi}\frac{\partial \omega^p}{\partial \xi}\right\} + \omega_\infty\left\{\frac{\partial \Psi}{\partial \xi}\frac{\partial T}{\partial \chi} - \frac{\partial \Psi}{\partial \chi}\frac{\partial T}{\partial \xi}\right\} = \frac{\omega'_\infty}{ReSc}\hat{\rho}^2\frac{\partial^2 T}{\partial \xi^2}, \tag{17}$$

$$\frac{\partial \Psi}{\partial \xi}\frac{\partial^2 \Psi}{\partial \chi \partial \xi} - \frac{\partial \Psi}{\partial \chi}\frac{\partial^2 \Psi}{\partial \xi^2} = \frac{\hat{\rho}}{Re}\frac{\partial^3 \Psi}{\partial \xi^3}, \tag{18}$$

$$(1 + R\hat{\rho}\omega^p C^p)\left\{\frac{\partial \Psi}{\partial \xi}\frac{\partial T}{\partial \chi} - \frac{\partial \Psi}{\partial \chi}\frac{\partial T}{\partial \xi}\right\} - \frac{\omega_\infty \hat{\rho}^2}{ReSc}(C^v - C^g)\left(\frac{\partial T}{\partial \xi}\right)^2 + REv\left\{\frac{\partial \Psi}{\partial \xi}\frac{\partial \omega^p}{\partial \chi} - \frac{\partial \Psi}{\partial \chi}\frac{\partial \omega^p}{\partial \xi}\right\} = \frac{\hat{\rho}^2}{RePr}\frac{\partial^2 T}{\partial \xi^2}, \tag{19}$$

$$\hat{\rho} = (1 - \tilde{R}\omega^p)^{-1}. \tag{20}$$

Although the respective equations governing the higher order terms in the expansion (15) may be obtained by a systematic mathematical procedure, the primary effect, which is shown in the terms of order $(\lambda^*/L^*)^0$, is of interest here. The equations of the basic problem imply the case of rapidly evaporating drops and locally saturated mixture throughout the two phase region. That is, the local vapor concentration and mixture temperature are related through phase-equilibrium, approximated here by the vapor pressure relation for the liquid. The terms involving derivatives of temperature in equation (17) form a mass generation term for the particles. The ratio of thermal to mass diffusivity determines whether particles evaporate throughout the two phase region or grow in the region of the boundary layer far from the wall due to supersaturation and ultimately evaporate nearer the wall.

The dry wall condition implies the presence of a finite region of gas phase only next to the wall. The thickness of this region, $\delta(x)$, unknown *a priori*, is determined as part of the solution. While the outer region is described by equations (16)–(20), the inner region is described by the following well-known single-phase equations which are obtained from equations (1)–(5) in the limit as $R \to 0$.

$$\frac{\partial \Psi_i}{\partial \xi}\frac{\partial \omega_i}{\partial \chi} - \frac{\partial \Psi_i}{\partial \chi}\frac{\partial \omega_i}{\partial \xi} = \frac{1}{ReSc}\frac{\partial^2 \omega i}{\partial \xi^2}, \tag{21}$$

$$\frac{\partial \Psi_i}{\partial \xi}\frac{\partial^2 \Psi_i}{\partial \chi \partial \xi} - \frac{\partial \Psi_i}{\partial \chi}\frac{\partial^2 \Psi_i}{\partial \xi^2} = \frac{1}{Re}\frac{\partial^3 \Psi_i}{\partial \xi^3}, \tag{22}$$

$$\frac{\partial \Psi_i}{\partial \xi}\frac{\partial T_i}{\partial \chi} - \frac{\partial \Psi_i}{\partial \chi}\frac{\partial T_i}{\partial \xi} = \frac{1}{RePr}\frac{\partial^2 T_i}{\partial \xi^2}. \quad (23)$$

Having arrived at a two region formulation, additional conditions at the interface must be written. The additional variable, $\delta(x)$, is determined as the location where saturation conditions in the two phase region can no longer be satisfied. In general, this implies that drop mass concentration vanishes discontinuously at $\delta(x)$, consistent with the possibility of infinite evaporation rate for particles of vanishing size. The appropriate interface conditions at $\delta(x)$ are then as follows:

Conservation of mixture mass,

$$\frac{\partial \Psi}{\partial \xi}\frac{\mathrm{d}\xi_\delta}{\mathrm{d}\chi} + \frac{\partial \Psi}{\partial \chi} = \frac{\partial \Psi_i}{\partial \xi}\frac{\mathrm{d}\xi_\delta}{\mathrm{d}\chi} + \frac{\partial \Psi_i}{\partial \chi}, \quad (24)$$

where ξ_δ, denoting the transformed inner layer thickness, is a function of χ only;

Conservation of thermal energy,

$$\omega^p REv\left\{\frac{\partial \Psi}{\partial \xi}\frac{\mathrm{d}\xi_\delta}{\mathrm{d}\chi} + \frac{\partial \Psi}{\partial \chi}\right\} = \frac{1}{RePr}\left\{\frac{\partial T_i}{\partial \xi} - \hat{\rho}\frac{\partial T}{\partial \xi}\right\}. \quad (25)$$

Continuity of velocity, shear and temperature,

$$\frac{\partial \Psi}{\partial \xi} = \frac{\partial \Psi_i}{\partial \xi}, \quad \hat{\rho}\frac{\partial^2 \Psi}{\partial \xi^2} = \frac{\partial^2 \Psi_i}{\partial \xi^2}, \quad T = T_i. \quad (26)$$

Conservation of mass–liquid and vapor,

$$\{\omega + R\hat{\rho}\omega^p\}\left\{\frac{\partial \Psi}{\partial \xi}\frac{\mathrm{d}\xi_\delta}{\mathrm{d}\chi} + \frac{\partial \Psi}{\partial \chi}\right\} - \omega\hat{\rho}\left\{\frac{\partial \Psi_i}{\partial \xi}\frac{\mathrm{d}\xi_\delta}{\mathrm{d}\chi} + \frac{\partial \Psi_i}{\partial \chi}\right\} + \frac{\hat{\rho}}{RePr}\left\{\omega_\infty\hat{\rho}\frac{\partial T}{\partial \xi} - \frac{\partial \omega_i}{\partial \xi}\right\} = 0. \quad (27)$$

The wall conditions, equations (10), apply to the solution in the inner region and are given in the transformed variables as

$$\frac{\partial \Psi_i}{\partial \xi}(\chi, 0) = \frac{\partial \Psi_i}{\partial \chi}(\chi, 0) = \frac{\partial \omega_i}{\partial \xi}(\chi, 0) = T_i(\chi, 0) = 0, \quad (28)$$

while free stream conditions, equations (11), apply to the solution in the outer region

$$\lim_{y\to\infty}\frac{\partial \Psi}{\partial \xi}(\chi, \xi) = \lim_{y\to\infty} T(\chi, \xi) = 1,$$

$$\lim_{y\to\infty}\omega^p(\chi, \xi) = \frac{1}{1 + \tilde{R}}. \quad (29)$$

The above partial differential equations subject to the imposed boundary conditions are reduced to a set of coupled ordinary differential equations with corresponding boundary conditions by the following similarity transformation,

$$\Psi(\chi, \xi) = \left\{\frac{v^*\chi}{u_\infty^* L^*}\right\}^{\frac{1}{2}} f(\eta), \quad T(\chi, \xi) = \theta(\eta),$$

$$\omega^p(\chi, \xi) = g(\eta), \quad \omega(\chi, \xi) = h(\eta), \quad (30)$$

$$\eta(\chi, \xi) = \xi\left\{\frac{u_\infty^* L^*}{v^*\chi}\right\}^{\frac{1}{2}}$$

The transformed equations for the inner region become

$$f_i''' + \tfrac{1}{2} f_i f_i'' = 0, \quad (31)$$

$$\theta_i'' + \frac{Pr}{2} f_i\theta_i' = 0, \quad (32)$$

$$h_i'' + \frac{Sc}{2} f_i h_i' = 0, \quad (33)$$

and, for the outer region,

$$f''' + \frac{1}{2\hat{\rho}} ff'' = 0, \quad (34)$$

$$g' - S_1\theta' + \frac{2S_2}{fSc}(\theta'\hat{\rho}) = 0, \quad (35)$$

$$\theta'' + \frac{Pr}{2}\frac{E_1}{\hat{\rho}^2} f\theta' + LuE_2(\theta')^2 = 0, \quad (36)$$

$$\hat{\rho} = (1 - \tilde{R}g)^{-1}. \quad (37)$$

where the variable coefficients S_1, S_2, E_1, E_2 are given in the appendix. The boundary conditions transform as follows:

$$\eta = 0: f_i = f_i' = \theta_i = h_i' = 0, \quad (38)$$

$$\eta \to \infty : f' = \theta' = 1, \quad g = (1 + \tilde{R})^{-1}, \tag{39}$$

$$\eta = \eta_\delta : f = f_i, \quad f' = f_i', \quad f'' = \frac{1}{\hat{\rho}} f_i'',$$

$$\theta = \theta_i, \quad h = h_i,$$

$$\theta' - \{\theta_i' - PrREvf\omega^p/2\}/\hat{\rho} = 0, \tag{40}$$

$$(1 - \hat{\rho})\{\omega_\infty + \omega_\infty'(T - 1)\} + R\hat{\rho}\omega^p + \frac{2\hat{\rho}}{fSc}\{\omega_\infty \hat{\rho}\theta' - h_i\} = 0.$$

Solving equation (33) gives a uniform vapor concentration in the inner region. The two point boundary value problem posed by the remaining equations (31), (32), (34)–(37) subject to the boundary conditions (38), (39) and (40), was solved as an initial value problem. Wall conditions and inner region thickness were assumed for the unknown values. The numerical integration employed the fourth order Runge–Kutta method in conjunction with a matrix Newton–Raphson routine to converge to the correct wall conditions and inner layer thickness. Limits on trial solution excursions [12] substantially speeded convergence and made the solution technique virtually independent of the assumed wall conditions. Details of the solution as well as other details of the study may be found elsewhere [13].

The wall heat flux and shear stress are given in terms of the gradient of the temperature and velocity profiles, respectively, at the wall,

$$q^* = -k^* \frac{\partial u^*(x^*, 0)}{\partial y^*}, \tag{41}$$

$$\tau^* = -\mu^* \frac{\partial u^*(x^*, 0)}{\partial y^*}. \tag{42}$$

The local heat transfer coefficient is computed using the relation,

$$h^* = \frac{q^*}{(T_w^* - T_\infty^*)}, \tag{43}$$

and the local values of Nusselt number and dimensionless wall shear are given by

$$Nu = \frac{h^* x^*}{k^*} = \frac{d\theta(0)}{d\eta} \tilde{R}e^{\frac{1}{2}}. \tag{44}$$

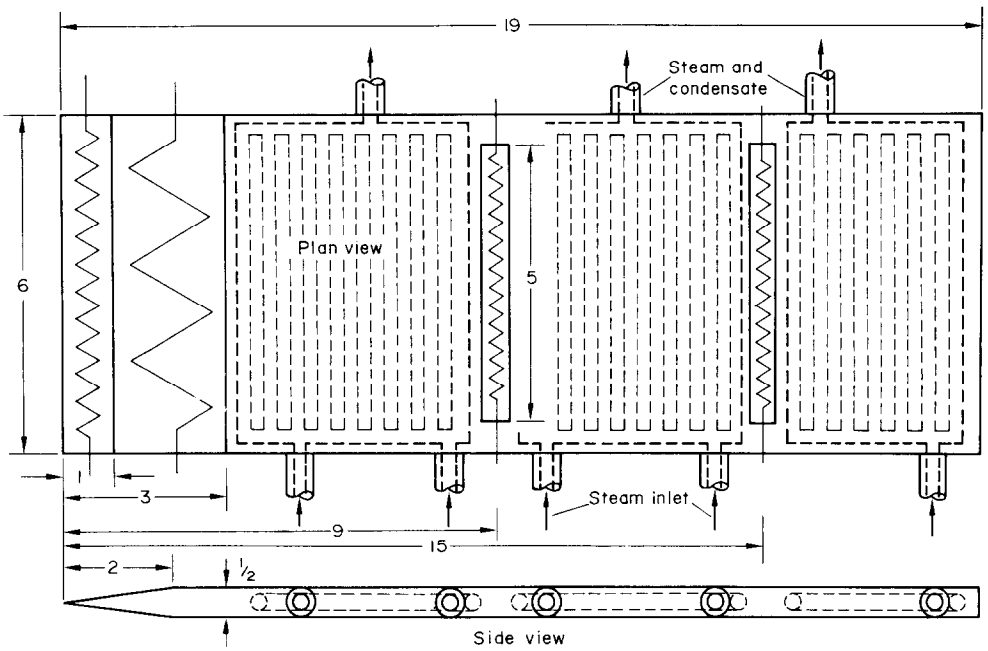

FIG. 1. Test surface layout.
Dimensions in inches.
Electrical resistance heater ~~~~~

$$\tau^*/\rho^* u_\infty^* = \frac{df(0)}{d\eta}\tilde{R}e^{-\frac{1}{2}}. \quad (45)$$

EXPERIMENT

The local heat flux was measured on an isothermal surface in a zero pressure gradient mist flow composed of an air/water vapor gas phase with water particles. The mist was generated with pneumatic nozzles, including an ultrasonic generator, in the plenum of a wind tunnel especially constructed for mist containment. All but the very smallest drops settled out of the mist in the low velocity plenum, where turbulence also was attenuated.

The test surface, shown in Fig. 1, was based on a previous design [14]. However, both sides of the surface were used in this case for heat transfer to the flow to circumvent the problem of insulating one side. The plate was machined from 2024-T351 aluminum and was heated using a natural circulation boiler system in which steam condensed in holes drilled through the plate normal to the direction of external mist flow. Steady flow of steam through the test plate was insured by the use of an additional condenser in the loop after the plate with capacity greater than plate capacity. In addition, electrical heaters were incorporated into the leading edge area to supply the excess power required there to maintain isothermal conditions. The leading edge was sanded to a $\frac{1}{64}$ in. radius and was smoothly contoured into the flat surface.

The two test heaters providing the local heat flux data were $\frac{1}{2} \times \frac{1}{2} \times 5$ in. aluminum blocks heated with electrical resistance elements located in holes drilled inside the blocks. The units were located 9 in. (test heater 1) and 15 in. (test heater 2) from the leading edge in sections cut completely through the interior of the steam heated plate, dissipating heat to the mist flow on both sides. Teflon insulation strips isolated the test heater thermally from the steam heated plate which also served as a guard heater. Each joint was sanded smooth on the surface.

In operation, the boiler power and secondary condenser cooling rate were adjusted to give the desired plate temperature. Then, power to the leading edge and test heaters was adjusted such that temperature differences between test heaters and surrounding plate locations were less than 1°F. Thermocouples in the leading edge area indicated temperatures within $\pm 1\frac{1}{2}$°F of the mean plate value. Test heater power measurements, corrected for lead resistance and plate radiation loss, were then divided by twice the test heater corrected surface area to give the local heat flux, q^*. The experimental values of heat transfer coefficient were calculated using equations (43) and (44). Error analysis by both experimental and analytical means indicated an uncertainty in experimental Nusselt number of approximately ± 4 per cent at the high values and ± 8 per cent at the low values.

The water content in the mist was determined through measurement of water flow rate into the nozzles, measurement of settling rate out of the plenum, and calculation of the liquid which evaporated to saturate the intake tunnel air. A water mass balance applied to the tunnel under steady operation then yielded the mass flow rate of liquid in the mist, and thus the liquid mass fraction, with an experimental uncertainty of the order ± 5 per cent at higher tunnel velocity, increasing to ± 22 per cent at lower velocity. Based upon calculations of drop settling rate and residence time in the plenum, the estimated maximum drop size in the mist was 3 μ, resulting in a maximum experimental λ^*/L^* value of 0·048.

RESULTS AND DISCUSSION

Theoretical velocity and temperature distributions are shown in Fig. 2 for selected values of the free stream liquid mass ratio represented by R. The limiting case $R = 0$ corresponds to a single phase gas boundary layer. The other parameters, which are kept constant, are typical of a water mist in air at atmospheric conditions. The vapor concentration may be determined immediately from the local temperature using

Table 2. Wall Nusselt number and dimensionless shear

R	0·000	0·005	0·010	0·015	0·020	0·060	0·100
$Nu/\tilde{R}e^{\frac{1}{2}}$	0·295	0·316	0·332	0·346	0·359	0·429	0·475
$\tau^*/\rho^* u_\infty^{*2}/\tilde{R}e^{-\frac{1}{2}}$	0·332	0·332	0·332	0·332	0·333	0·335	0·339

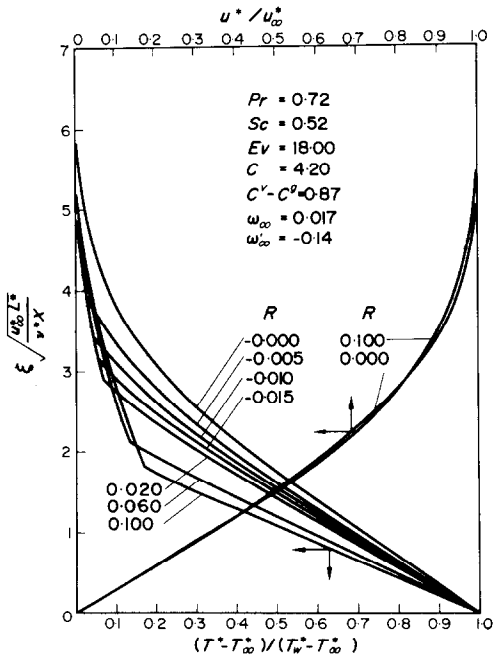

FIG. 2. Temperature and velocity distributions.

equation (8) in the outer region, while it remains constant at the interface value in the inner region. For parameter values characteristic of an air/water vapor mixture, the liquid mass concentration exhibits negligible change in the outer region, ultimately vanishing at the interface surface and causing the noticeable corner in the temperature profile due to the energy absorption upon evaporation. An increasing content of free stream liquid forces the two phase region closer to the hot wall, as shown by the decreasing values of η_δ.† This results from the increase of energy absorbed upon particle evaporation in the two phase region and at the interface. The temperature at a given position in the boundary layer thus decreases with increasing R, leading to an increase in wall temperature gradient and heat transfer.

While the second phase has a significant effect on the temperature distribution, the effect on velocity distribution and wall shear is negligible. This result is not surprising since the maximum variation in mixture density was 1 per cent at the free stream liquid contents investigated. In contrast, the effect of liquid concentration on temperature is greatly magnified by the enthalpy of evaporation, resulting in a large absorption of heat during phase change. Calculations verified that velocity and temperature distributions approach the single phase values as $R \to 0$.

Analytical values of $Nu/\tilde{R}e^{\frac{1}{2}}$ and

$$\tau^*/\rho^* u_\infty^{*2}/\tilde{R}e^{-\frac{1}{2}}$$

are given in Table 2 for selected values of R, indicating the effect of liquid content.

The local Nusselt number is seen to increase as R increases above zero, the limiting case of single phase flow. The effect of R on wall shear, however, is seen to be negligible. Dependence of the local Nusselt number and dimensionless wall shear on $\tilde{R}e^{-\frac{1}{2}}$ and $\tilde{R}e^{-\frac{1}{2}}$ respectively, a characteristic of single phase laminar boundary layers, is preserved in the present two phase flow solution to the first order.

The agreement between experimentally determined values of Nu and the theory is shown in Fig. 3, for selected values of R. Within the experimental scatter, the data indicates an increase in Nu with increasing R and dependence of Nu on $\tilde{R}e^{\frac{1}{2}}$. A set of data for $R = 0$ is included as a reference. The surface heat transfer in mist flow is seen to be increased above that in single

† Research is being currently pursued by the first author to investigate the conditions for which the inner layer thickness approaches zero and the resulting transition between the dry wall regime and liquid film regime.

phase gas flow by a maximum of 15 per cent at the maximum liquid mist content investigated. The Reynolds number dependence of the experimental data also indicates that the observed increase in heat transfer is due to the second phase in a laminar flow rather than a turbulence effect.

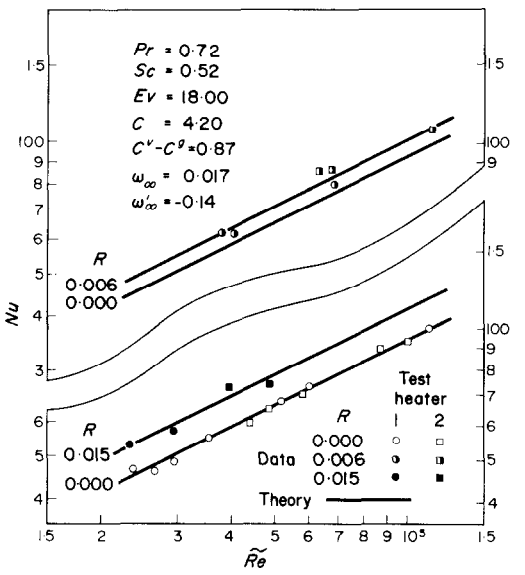

FIG. 3. Theoretical and experimental Nusselt number.

ACKNOWLEDGEMENTS

The authors wish to acknowledge Professor V. S. Arpaci who proposed the research, Professor R. B. Keller for guidance in the experimental program, and the National Science Foundation and Horace H. Rackham School of Graduate Studies for fellowship support.

REFERENCES

1. F. E. MARBLE, Dynamics of a gas containing small solid particles, *Fifth AGARD Combustion and Propulsion Colloquium*, p. 175. Macmillan, New York (1963).
2. R. E. SINGLETON, The compressible gas–solid particle flow over a semi-infinite flat plate, *Z. Angew. Math. Phys.* **16**, 421–449 (1965).
3. S. L. SOO, *Fluid Dynamics of Multiphase Systems*. Blaisdell, Waltham (1967).
4. J. W. HODGSON, R. T. SATERBAK and J. E. SUNDERLAND, An experimental investigation of heat transfer from a spray cooled isothermal cylinder, *J. Heat Transfer* **90**, 457–463 (1968).
5. R. L. MEDNICK and C. P. COLVER, Heat transfer from a cylinder in an air–water spray flow stream, *A.I.Ch.E. Jl* **15**, 357–362 (1969).
6. J. E. SMITH, Heat transfer studies of water-spray flows, ARL Report No. 66-0091 (1966).
7. M. E. GOLDSTEIN, WEN-JAI YANG and J. A. CLARK, Momentum and heat transfer in laminar flow of a gas with liquid-droplet suspension over a circular cylinder, *J. Heat Transfer* **89**, 185–193 (1967).
8. L. S. TONG, *Boiling Heat Transfer and Two-Phase Flow*. Wiley, New York (1965).
9. R. D. CESS and E. M. SPARROW, Film boiling in a forced convection boundary-layer flow, *J. Heat Transfer* **83**, 370–376 (1961).
10. A. H. SHAPIRO and A. J. ERICKSON, On the changing size spectrum of particle clouds undergoing evaporation, combustion, or acceleration, *Trans Am. Soc. Mech. Engrs* **79**, 775–788 (1957).
11. S. I. PAI, *Viscous Flow Theory. I—Laminar Flow*. Van Nostrand, Princeton (1956).
12. A. M. O. SMITH and D. W. CLUTTER, Machine calculation at compressible laminar boundary layers, *AIAA Jl* **3**, 639–647 (1965).
13. J. W. HEYT, The laminar boundary layer in two component mist flow, Ph.D. Thesis, University of Michigan, Ann Arbor, Michigan (1968).
14. J. KESTIN, P. F. MAEDER and H. E. WANG, Influence of turbulence on the transfer of heat from plates with and without a pressure gradient, *Int. J. Heat Mass Transfer* **3**, 133–154 (1961).

APPENDIX

The variable coefficients appearing in equations (35) and (36) are as follows,

$$S_1 = -\frac{\omega'_\infty\{1 - Lu - R\hat{\rho}gLuC^p\}}{R\hat{\rho}\{1 - \omega_\infty - \omega'_\infty(T-1)\} - \omega'_\infty REvLu}, \quad (A.1)$$

$$S_2 = -\frac{(\omega'_\infty)^2(C^v - C^g)Lu}{R\hat{\rho}\{1 - \omega_\infty - \omega'_\infty(T-1)\} - \omega'_\infty REvLu}, \quad (A.2)$$

$$E_1 = \frac{R\hat{\rho}(1 + R\hat{\rho}gC^p)\{1 - \omega_\infty - \omega'_\infty(T-1)\} - \omega'_\infty REv}{R\hat{\rho}\{1 - \omega_\infty - \omega'_\infty(T-1)\} - \omega'_\infty REvLu}, \quad (A.3)$$

$$E_2 = \frac{\omega'_\infty(C^v - C^g)R\hat{\rho}\{1 - \omega_\infty - \omega'_\infty(T-1)\}}{R\hat{\rho}\{1 - \omega_\infty - \omega'_\infty(T-1)\} - \omega'_\infty REvLu}. \quad (A.4)$$

The vapor pressure curve of the liquid is linearized to give

$$\omega_s = \omega_\infty + \omega'_\infty(T^p - T_\infty), \quad (A.5)$$

where $\omega'_\infty = \partial\omega_s/\partial T^p$ is evaluated at the free stream conditions, and ω_s is the vapor concentration of saturated air at the local liquid temperature. The assumption of quasi-steady evaporation results in the following equation for wet bulb depression,

$$(T - T^p) = -EvLu(\omega_s - \omega). \quad (A.6)$$

Simultaneous solution of equations (A.5) and (A.6) then gives equation (8) with the constants

$$C_1 = \frac{EvLu}{1 - \omega'_\infty EvLu}\{\omega'_\infty - \omega_\infty\}, \tag{A.7}$$

$$C_2 = -\frac{\omega'_\infty EvLu}{1 - \omega'_\infty EvLu}, \tag{A.8}$$

$$C_3 = \frac{EvLu}{1 - \omega'_\infty EvLu}. \tag{A.9}$$

TRANSFERT THERMIQUE POUR UN ÉCOULEMENT BINAIRE DE BROUILLARD

Résumé—La convection forcée en couche limite laminaire comportant un gaz à deux composants avec des particules liquides dispersées passant sur une surface sèche isotherme est étudiée théoriquement et expérimentalement. L'effet de la présence des particules et de leur évaporation sur la surface, du transfert thermique et du frottement pariétal est déterminé pour le cas limite de concentrations diluées de petites particules ayant une grande vitesse d'évaporation. Les solutions tiennent compte des distributions de vitesse, de température, de vapeur et de liquide à travers la couche limite et de l'existence d'une région près de la paroi sans particules à cause de l'évaporation complète. Il est montré qu'un accroissement de la proportion de liquide augmente sensiblement le transfert thermique pariétal sans modifier le frottement pariétal. Les résultats théoriques coordonnent les mesures de transfert thermique pour un écoulement contenant air, vapeur d'eau et particules d'eau liquide.

DER WÄRMEÜBERGANG BEI DER ZWEISTOFF-NEBELSTRÖMUNG

Zusammenfassung—Die laminare Grenzschicht bei der erzwungenen Konvektion für ein Zweikomponentengas mit fein verteilten Flüssigkeitströpfchen über einer trockenen isothermen Oberfläche wird analytisch und experimentell untersucht. Der Einfluss der Anwesenheit von Flüssigkeitsteilchen und der Verdampfung auf die Grenzschichtstruktur, den Wärmeübergang und die Scherkräfte an der Wand werden für den Grenzfall stark verdünnter Konzentrationen von kleinen Teilchen mit einer hohen Verdampfungsrate bestimmt. Die Lösungen enthalten die Geschwindigkeits-, Temperatur-, Dampf- und Flüssigkeitsverteilungen über die Grenzschicht und im Bereich nahe der Wand, der wegen der vollständigen Verdampfung frei von Flüssigkeitsteilchen ist. Es wird gezeigt, dass für einen steigenden Freistromflüssigkeitsgehalt der Wärmeübergang an der Wand wesentlich ansteigt, während das Anwachsen der Scherkräfte vernachlässigbar ist. Theoretische Ergebnisse korrelieren die Wärmeübergangsmessungen an der Wand für eine Luft/Wasserdampf, Wasserteilchen-Nebelströmung.

ТЕПЛОПЕРЕНОС К ТЕЧЕНИЮ КАПЕЛЕК В ПОГРАНИЧНОМ СЛОЕ

Аннотация—Теоретически и экспериментально изучался ламинарный пограничный слой на сухой изотермической поверхности при вынужденном течении двухкомпонентного газа, содержащего диспергированные в нем жидкие частицы. Определено влияние наличия частиц и испарения на структуру пограничного слоя, теплообмен и сдвиговое напряжение на стенке для предельного случая слабых концентраций мелких частиц с большой скоростью испарения. Решения включают распределение скорости, температуры пара и жидкости в пограничном слое раствора, а также увеличение области, свободной от частичек, благодаря полному испарению. Показано, что при возрастании содержания жидкости в свободном потоке увеличение теплообмена тепловых потоков на стенке существенно, тогда как увеличение напряжения трения на стенке незначительно. Получены теоретические зависимости для теплообмена стенки с потоком смеси воздуха с водяным паром, содержащей взвешенные капельки воды.